TOR regulates the subcellular distribution of DIM2, a KH domain protein required for cotranscriptional ribosome assembly and pre-40S ribosome export

EMMANUEL VANROBAYS,[1,3,4] ALEXIS LEPLUS,[1,3] YVONNE N. OSHEIM,[2] ANN L. BEYER,[2] LUDIVINE WACHEUL,[1] and DENIS L.J. LAFONTAINE[1]

[1]Fonds de la Recherche Scientifique (FRS-FNRS), Académie Wallonie-Bruxelles, Institut de Biologie et de Médecine Moléculaires, Université Libre de Bruxelles, Charleroi-Gosselies, B-6041, Belgium
[2]Department of Microbiology, University of Virginia Health System, Charlottesville, Virginia 22908-0734, USA

ABSTRACT

Eukaryotic ribosome synthesis is a highly dynamic process that involves the transient association of scores of *trans*-acting factors to nascent pre-ribosomes. Many ribosome synthesis factors are nucleocytoplasmic shuttling proteins that engage the assembly pathway at early nucleolar stages and escort pre-ribosomes to the nucleoplasm and/or the cytoplasm. Here, we report that two 40S ribosome synthesis factors, the KH-domain protein DIM2 and the HEAT-repeats/Armadillo-domain and export factor RRP12, are nucleolar restricted upon nutritional, osmotic, and oxidative stress. Nucleolar entrapment of DIM2 and RRP12 was triggered by rapamycin treatment and was under the strict control of the target of rapamycin (TOR) signaling cascade. DIM2 binds pre-rRNAs directly through its KH domain at the 5′-end of ITS1 (D-A$_2$ segment) and, consistent with its requirements in early nucleolar pre-rRNA processing, is required for efficient cotranscriptional ribosome assembly. The substitution of a single and highly conserved amino acid (G207A) within the KH motif is sufficient to inhibit pre-rRNA processing in a fashion similar to genetic depletion of DIM2. DIM2 carries an evolutionarily conserved putative nuclear export sequence (NES) at its carboxyl-terminal end that is required for efficient pre-40S ribosome export. Strikingly, DIM2 and RRP12 are both involved in the nucleocytoplasmic translocation of pre-ribosomes, suggesting that this step in the ribosome assembly pathway has been selected as a regulatory target for the TOR pathway.

Keywords: ribosome synthesis; pre-rRNA processing; ribosome export, target of rapamycin (TOR), KH domain, nucleolus

INTRODUCTION

Ribosome assembly is a complex and highly dynamic process that initiates cotranscriptionally with the transient association to the nascent transcripts of scores of ribosome synthesis factors and the faithful incorporation of ribosomal proteins. This results in the constant compositional and structural remodeling of nascent pre-ribosomes. Concomitantly with these assembly reactions, pre-rRNAs are processed (mature rRNAs are released from precursors RNAs) and extensively modified (specific residues are selected for 2′-O- ribose methylation, base methylation, and pseudouridine formation) (for reviews, see Fatica and Tollervey 2002; Fromont-Racine et al. 2003; Henras et al. 2008). Strikingly, many ribosome synthesis factors are nucleocytoplasmic shuttling proteins that engage the assembly pathway at early nucleolar stages, escort pre-ribosomes along their maturation course through the nucleoplasm, the nuclear pore complexes (NPC), and into the cytoplasm. The KH-domain containing protein DIM2 (YOR145C) is one such *trans*-acting factor and, as known, functions in the nucleolus and the cytoplasm (Senapin et al. 2003; Vanrobays et al. 2004). Indeed, DIM2 is required for early nucleolar pre-rRNA processing and late cytoplasmic pre-rRNA methylation and is associated with nascent transcripts and cytoplasmic pre-rRNAs. The synthesis of ribosomal components in equimolar amounts entails extensive coordination and integration and is under the tight control of regulatory cascades such as the target of rapamycin (TOR), which provides nutrient-related growth control (for reviews,

---

[3]These authors contributed equally to this work.
[4]**Present address:** Cancer Research UK, London WC2A 3PX, UK.
Reprint requests to: Denis L.J. Lafontaine, Fonds de la Recherche Scientifique (FRS-FNRS), Académie Wallonie-Bruxelles, Institut de Biologie et de Médecine Moléculaires, Université Libre de Bruxelles, rue des Professeurs Jeener et Brachet, 12, B-6041 Charleroi-Gosselies, Belgium; e-mail: denis.lafontaine@ulb.ac.be; fax: +3226509747.

Article published online ahead of print. Article and publication date are at http://www.rnajournal.org/cgi/doi/10.1261/rna.1176708.

see Jorgensen et al. 2004; Loewith and Hall 2004). The nucleo-cytoplasmic shuttling of DIM2 is tightly regulated by growth (Vanrobays et al. 2004), but what triggers its dynamic subcellular trafficking is currently not known.

Ribosome export is an active process that requires a karyopherin of the β family (the HEAT repeats CRM1/XPO1), a nuclear export sequence (NES)-containing adaptor, the RanGTP cycle, and specific nucleoporins (NUPs) (for reviews, see Tschochner and Hurt 2003; Zemp and Kutay 2007). License for pre-60S export is provided by the NES adaptor NMD3, which interacts with CRM1 (Ho et al. 2000; Gadal et al. 2001). In yeast, the nuclear mRNA export receptor MEX67-MTR2, which interacts directly with the NPC, provides an alternative, RanGTP-independent, pre-60S ribosome export pathway (Yao et al. 2007). It is likely that NMD3-CRM1, MEX67-MTR2, and possibly other adaptors such as ARX1 bind distinct sites on pre-60S ribosomes, providing synergistic interactions with the FG repeats of the nucleoporins during passage through the NPC (Lebreton et al. 2006; Bradatsch et al. 2007; Yao et al. 2007, 2008; Hung et al. 2008). Roughly one-third of all NPC proteins contain various hydrophobic FG repeat domains that are highly unstructured or natively unfolded and are thought to line the inner surface of the NPC channel (for review, see Weis 2007). All known nuclear transport receptors can bind to FG-repeats-containing NUPs, and interactions between transport receptors and FG repeats are essential for translocation through the NPC. Export of pre-40S ribosomes is also dependent on CRM1 and likely involves multiple export adaptors. A contributor is the nonessential and NES-containing protein LTV1 (Seiser et al. 2006). In addition, many ribosome synthesis factors have been involved in subunit export, e.g., the HEAT repeats/Armadillo RRP12 that participates in the export of both subunits through presumed interactions with nucleoporins (Oeffinger et al. 2004).

Here, we report that under starvation and stressful growth conditions, the 40S ribosome synthesis factors DIM2 (RRP20/PNO1) and RRP12 specifically concentrate within the nucleolus in a rapamycin-sensitive and TOR-dependent fashion. Further, DIM2 was found to bind pre-rRNAs directly at the D-A_2 spacer region through its KH domain. Finally, DIM2 is required for cotranscriptional ribosome assembly and carries an evolutionarily conserved putative NES sequence that is required for efficient pre-40S ribosome export.

RESULTS

The KH domain of DIM2 is required for early nucleolar pre-rRNA processing

DIM2 carries a conserved KH and putative RNA binding domain at its carboxyl-terminal end (Fig. 1A–C; Senapin et al. 2003; Vanrobays et al. 2004). Detailed blast analysis

and homology modeling indicated that the KH domain of DIM2 is of type I, corresponding to a motif of about 70 amino acid residues in length that exhibits the canonical $\beta1$-$\alpha1$-$\alpha2$-$\beta2$-$\beta3$-$\alpha3$ fold and the invariant GXXG central loop sequence (Grishin 2001). The RNA-binding groove is formed by the $\alpha1$ and $\alpha2$ helices, the GXXG loop, and the $\beta2$ strand (Lewis et al. 2000; Jia et al. 2007).

To test whether this domain is required for DIM2's functions, four mutations were generated: (1) a complete elimination of the KH domain (ΔKH, residues 179–252 missing); (2) a truncation of its most conserved and central region (ΔKH core, residues 203–213); (3) the introduction of a premature stop at position 203 (ΔC ter); and (4) the substitution of a single G residue for an alanine (G207A) (Fig. 1A–C). G207A was carefully selected by reference to described mutations at this conserved position that drastically impair the RNA-binding capability of other KH-domain-containing proteins (Jones and Schedl 1995; Garcia-Mena et al. 1999; Zhou et al. 2002).

Each mutation was expressed from a low-copy-plasmid as an amino-tagged Protein A (ProtA) construct and tested for its effects on growth and pre-rRNA processing in *tet::dim2* cells following depletion of endogenous chromosome-encoded DIM2 (addition of doxycycline) (Figs. 1, 2). Anti-ProtA Western-blotting analysis established that each construct was stably expressed and generated a fusion protein of the expected size (Fig. 1D). None of the three DIM2 truncations was capable of complementing *tet::dim2* cells for growth upon transfer to doxycycline-containing medium (Fig. 1D). The G207A substitution showed partial complementation but severely impacted growth (3.5-fold reduction). As a control, *tet::dim2* cells were transformed with a plasmid expressing a wild-type ProtA-DIM2 fusion and an empty control plasmid; the wild-type ProtA construct fully complemented growth (Fig. 1D).

Total RNA was extracted from cells grown in the absence of doxycycline and following depletion (+DOX) for up to 22 h. In the absence of complementing DIM2, pre-rRNA processing was primarily inhibited at the early nucleolar cleavage sites A_1 and A_2, resulting in the accumulation of a novel RNA (Fig. 2B, 22S, extending from A_0 to A_3), the concomitant disappearance of the 20S and $27SA_2$ pre-rRNAs, and a concurrent inhibition in 18S rRNA synthesis (Fig. 2A, cf. lanes 1–3 and 4–6; Fig. 2B). All three truncations inhibited pre-rRNA processing in a fashion similar to that which occurred upon DIM2 depletion (Fig. 2A, cf. lanes 1–3 and 7–15; Vanrobays et al. 2004). The G207A mutation was sufficient to inhibit pre-rRNA processing at sites A_1 and A_2, leading to a strong accumulation of the 22S RNA; however, in this case, and in agreement with the partial growth restoration, there was a persistent though reduced production of 20S and $27SA_2$ pre-rRNAs and 18S rRNA (Fig. 2A, lanes 16–18). Pre-rRNA processing in ITS2 was largely unaffected by mutations in the KH domain (Fig. 2A, panels III and IV; data not shown); this is as previously
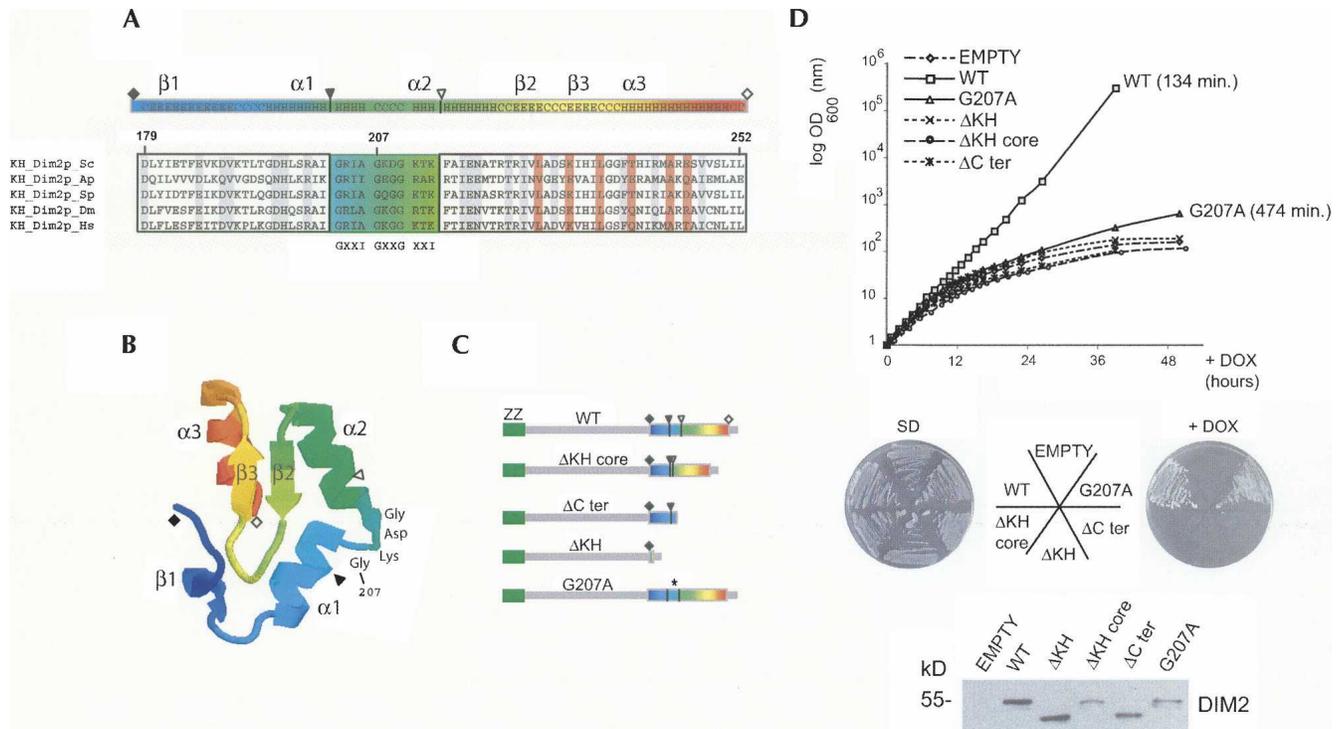
FIGURE 1. The KH domain of DIM2 adopts the canonical β1-α1-α2-β2-β3-α3 fold and is essential for protein function. (*A*) The KH domain of DIM2 is evolutionarily conserved. Sc, *Saccharomyces cerevisiae*; Ap, *Aeropyrum pernix*; Sp, *Schizosaccharomyces pombe*; Dm, *Drosophila melanogaster*; Hs, *Homo sapiens*. The KH domain extends from residue 179 to 252. The most conserved region (referred to here as "core domain") extends from residue 203 to 213; consensus (GXXIGXXGXXI; where X is any amino acid) shown at the *bottom*. The various regions of the KH domain are arbitrarily color-coded and annotated (closed and open diamonds and triangles) according to our functional mapping analysis (see below). Regions predicted to adopt helices (H), strands (E), and coils (C) are annotated. Residues conserved in KH domains are shaded in pink; identical or highly similar residues are highlighted in gray. (*B*) The three-dimensional structure of the KH domain of DIM2 was homology modeled based on the 1.5-Å resolution crystal structure of an archaeal homolog from *Aeropyrum pernix* (Jia et al. 2007; see Materials and Methods). Color code and annotations are as in panel *A*; central residues of the core subdomain are highlighted by their three-letter code. (*C*) Functional mapping of the KH domain. Each DIM2 construct was expressed from a low-copy (ARS/CEN-LEU2) plasmid as an amino-tagged Protein A fusion. The ΔKH core mutation carries an 11 amino acid deletion (residues 203–213). The ΔC ter mutation carries a premature stop codon at position 203. In the ΔKH allele, the whole KH domain encompassing residues 179–252 is deleted. The G207A mutation harbors a single amino acid substitution. (*D*) Steady-state levels of DIM2 constructs and effects of DIM2 mutations on growth. Each DIM2 mutation was tested for its effects on growth in liquid (*top* panel) and solid (*middle* panel) cultures in *tet::dim2* cells upon the addition of doxycycline. X axis, time of transfer to doxycycline (up to 48 h); Y axis, OD_{600}/OD_{600} at 0 min expressed in a log scale. The doubling time is indicated for the wild-type strain and the G207A substitution. SD, dextrose synthetic medium lacking leucine; +DOX, SD supplemented with 10 μg/mL of doxycycline. (*Bottom* panel) Each DIM2 construct was stably expressed. Equivalent amounts of total protein extracted in the absence of doxycycline-induced depletion were loaded in each lane and tested by anti-ProtA Western blot analysis.

reported upon DIM2 depletion (Senapin et al. 2003; Vanrobays et al. 2004). A difference was however noted in that at the late time point of depletion of 22 h, the ΔKH core and G207A mutations (Fig. 2A, lanes 9,18, respectively) accumulated a novel RNA that extended from site D to B_2 (data not shown). The D-B_2 RNA was previously reported in strains genetically depleted for Sm-like proteins and is indicative of alterations in pre-rRNA processing kinetics (Kufel et al. 2003).

The KH domain of DIM2 is required for pre-rRNA and pre-ribosome interaction in vitro and in vivo

Next, each mutation was evaluated for its effects on DIM2 interaction with RNA and association with the pre-ribosomes

(Fig. 3). Interaction with the RNA was tested in vivo by affinity purification and in vitro by gel-shift assays. Association with the pre-ribosomes was analyzed in velocity gradients.

Equivalent amounts of total extract prepared from cells expressing each mutation, the wild-type construct, or transformed with the empty plasmid were incubated with IgG-coupled agarose beads. Affinity-purified RNAs and proteins were analyzed by primer extension and by Northern and Western blotting (Fig. 3A). The wild-type construct efficiently coprecipitated the nucleolar 33S pre-rRNA (A_0 detection), the 20S pre-rRNA, and the cytoplasmic D-A_2 fragment. Importantly, this revealed that the D-A_2 segment of the pre-rRNAs is a primary binding site for DIM2. All three DIM2 truncations were severely impaired

for interaction with the RNAs. The ΔKH core mutation retained marginal interaction with the 33S pre-rRNA, though it and the other two truncations lost any significant interaction with the 20S pre-rRNA and the D-A_2 fragment (Fig. 3A, left panel). Strikingly, the G207A substitution maintained substantial interaction with large nucleolar pre-rRNAs but also lost association with the 20S pre-rRNA and its D-A_2 byproduct. As a control, the affinity-purified material was tested for the presence of the bait protein by anti-ProtA Western blotting; all constructs were efficiently recovered in the pellet fractions (Fig. 3A, right panel).

Full-length DIM2 and a version lacking the KH domain (ΔC ter) were expressed as GST fusions in bacteria, and increasing amounts of purified recombinant protein were incubated with identical quantities of gel-purified, in vitro-synthesized D-A_2 fragment (Fig. 3B; Materials and Methods). In the presence of full-length GST-DIM2, the radio-labeled RNA was significantly shifted to two positions in the gel (Fig. 3B, "*" and "**"). No such significant shifts were observed with the ΔC ter construct.

Finally, the interaction of the KH mutants with pre-ribosomes was tested in velocity gradients. An equivalent amount of total extract from cells expressing each mutation was loaded in 10%–30% glycerol gradients and resolved by high-speed centrifugation. Twenty fractions were recovered and total protein analyzed by anti-ProtA Western blotting (Fig. 3C). Wild-type DIM2 was detected in three distinct pools corresponding to 90S pre-ribosomes (faint bands in fraction 14 and upwards), pre-40S ribosomes (Fig. 3C, fractions 9–12) and the top of the gradient. All four mutant constructs lost interaction with pre-40S ribosomes. A low level of interaction with large pre-ribosomes was somehow sustained in the three truncations, although the particles were shifted to slower migrating fractions (Fig. 3C, centered around fractions 14,15), indicative of gross assembly defects. Strikingly, the G207A substitution maintained a substantial level of interaction with 90S pre-ribosomes. This observation is fully consistent with the affinity purification data set (Fig. 3A), the partial growth restoration (Fig. 1D), and the limited pre-rRNA processing inhibitions observed with the G207A mutation (Fig. 2A).

DIM2 is required for cotranscriptional ribosome assembly

A recent morphological study of yeast rRNA genes (Christmas trees) described reproducible cotranscriptional processing steps (Osheim et al. 2004), which are also seen in the representative control gene in Figure 4. The 5′-ends of nascent ribosomal transcripts are initially bound by small 5′-ETS particles or terminal knobs (Fig. 4, small gray particles), which most likely include the box C+D snoRNA U3. The 5′-ETS particles soon condense into large SSU processomes comprising most of the 18S rRNA sequence (Fig. 4, larger red particles). In fast growing yeast strains,

SSU-processome compaction is followed in ~50% of the molecules by cotranscriptional cleavage within ITS1 and small subunit release (Fig. 4, control gene). Since DIM2 is essential for early pre-rRNA processing, we anticipated that its depletion would strongly impact the kinetics of cotranscriptional assembly. This was tested directly by chromatin spreading in cells depleted for DIM2 for 17 h (Fig. 4, right panel; see Supplemental Fig. S1 for a semiquantitative analysis). In these conditions, pre-rRNA processing was severely inhibited (see Fig. 2A). In the absence of DIM2, substantial delays in 5′-terminal knob deposition and severe SSU-processome assembly defects were noted. When detected, large particles were present mainly on final transcripts and were usually in a loose configuration. In
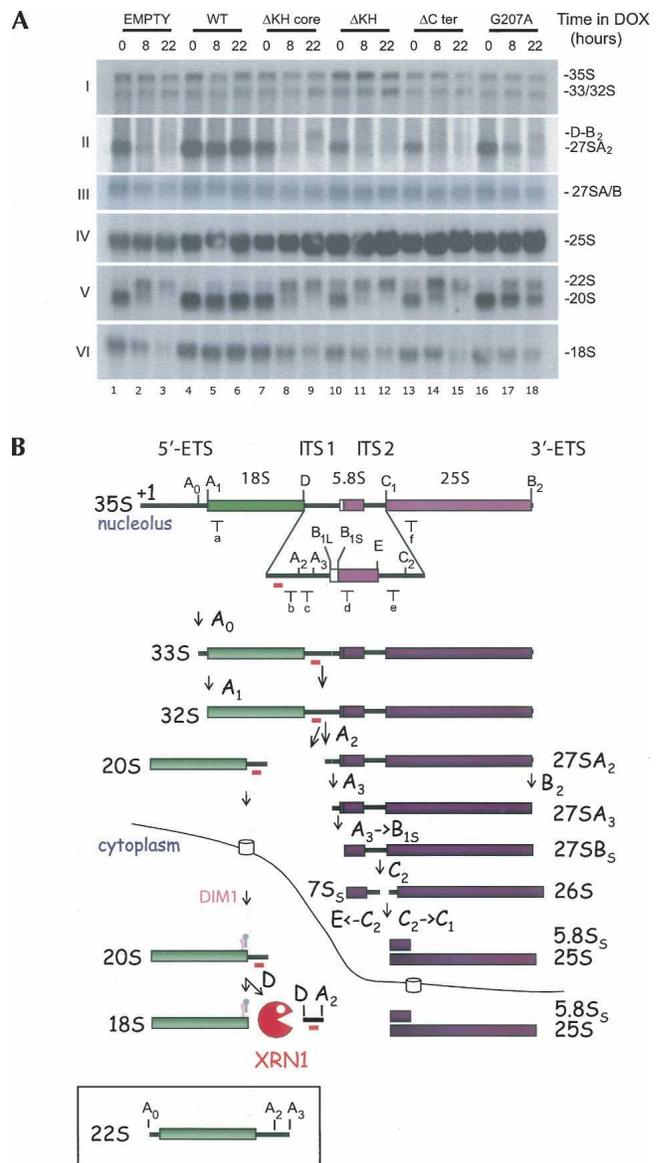

FIGURE 2. (Legend on next page)

addition, fewer transcripts, often with reduced protein levels, were detected, and normal cotranscriptional cleavage was absent, leading to the presence of extended and, on occasion, aberrantly cleaved transcripts.

DIM2 and RRP12 are concentrated within the nucleolus upon nutritional, osmotic, and oxidative stress

We previously reported that DIM2 is dynamically distributed since it is detected: (1) throughout the cells in fast-growing yeast; (2) restricted to the nucleus at the diauxic shift; and (3) exclusively localized to the nucleolus in saturated cultures (Vanrobays et al. 2004). Similar to DIM2, we found that RRP12, another 40S subunit synthesis factor, is specifically relocated to the nucleolus upon nutritional stress (Fig. 5A). Such a relocation to the nucleolus is not a generic trait and does not simply reflect the ribosome synthesis inhibitions that prevail in saturated cultures since it was not observed with 10 other 40S ribosome synthesis factors, including DIM1, ENP1, FAP7, HRR25, LTV1, NOB1, NOP6, RIO2, SLX9, and TSR1 (data not shown). For both DIM2 and RRP12, the nucleolar enrichment was readily reversible upon the addition of glucose or fresh medium to the cultures (Vanrobays et al. 2004; data not shown).

FIGURE 2. The KH domain of DIM2 is required for pre-rRNA processing at sites A_1 and A_2. (*A*) Pre-rRNA processing analysis. A single alanine substitution in the KH domain of DIM2 at the conserved position 207 (G207A) was sufficient to mimic the inhibitory effects on pre-rRNA processing of protein depletion. Steady-state levels of pre-rRNA and mature rRNA in *tet::dim2* cells transformed with the DIM2 constructs depicted in Figure 1C, as well as with an empty control plasmid, are shown. Total RNA was extracted from cells growing exponentially in selective medium (SD −leu) in the absence (0-h time points) or following the addition of doxycycline (8 and 22 h). Total RNA was separated on denaturing agarose gels and transferred to nylon membranes for Northern blotting. Oligonucleotides used in the hybridization are described in Supplemental Table 3 and in panel *B*. Panels I and V were hybridized with probe b, panel II with probe c, panels III with probe e, panel IV with probe f, and panel VI with probe a. (*B*) Primary Pol I transcript (35S) and simplified pre-rRNA processing pathway in *S. cerevisiae*. The mature 18S, 5.8S, and 25S rRNA are interspersed with external transcribed spacers (5′-ETS and 3′-ETS), as well as with internal transcribed spacers (ITS1 and ITS2). Cleavage sites (A_0 to E) are indicated, as are probes a to f used in the Northern blot hybridizations and primer extension analysis. The position of the probe used in the FISH analysis at the 5′ end of ITS1 is represented in red. Three initial nucleolar cleavages at sites A_0, A_1, and A_2 generate successively the 33S, the 32S, and the 20S and $27SA_2$ pre-rRNAs. The 20S pre-rRNA is exported to the cytoplasm, where it is dimethylated by DIM1 and cleaved at site D, generating mature 18S rRNA. The $27SA_2$ pre-rRNA undergoes two alternative processing pathways, only one of which—the major, accounting for up to 80% of total pre-rRNA processing—is represented here. Cleavage at site A_3 by RNAse MRP is followed by 5′–3′ exoribonucleolytic digestion by RAT1 and XRN1 to B_{1S}. Endonucleolytic cleavage at site C_2 in ITS2 is followed by C_2 to E digestion by the Exosome and C_2 to C_1 digestion by RAT1 and XRN1. A full description can be found in Lafontaine (2004) and Henras et al. (2008). (*Inset*) 22S RNA.

To test whether the relocation of DIM2 and RRP12 to the nucleolus is triggered by cues other than nutrient starvation, cells growing exponentially and expressing either DIM2-GFP or RRP12-GFP were submitted to various stresses, including treatments with NaCl, DTT, DMSO, and H_2O_2, and were imaged in live conditions (Fig. 5B,C). All of these stresses triggered, with specific kinetics, the accumulation of DIM2 and RRP12 in a crescent-like structure reminiscent of the nucleolar structure. That this structure indeed corresponded to the nucleolus was established on fixed material either by indirect immunofluorescence with specific detection of the prototypic nucleolar antigen NOP1 (fibrillarin) and/or by DAPI counterstaining (Fig. 5D; data not shown).

The nucleolar entrapment of DIM2 and RRP12 is under TOR control

Next, we tested whether the evolutionarily conserved TOR pathway that provides nutrient-related growth control and regulates ribosome synthesis at multiple levels (see Discussion) is involved in DIM2 and RRP12 subcellular trafficking (Fig. 6). The TOR pathway can be inhibited pharmacologically by treatment with the immunosuppressive drug rapamycin or genetically by specific mutations. Treating yeast cells with rapamycin elicits many physiological changes that bear similarity to cellular responses to nutrient starvation. Wild-type cells (TOR1) expressing DIM2-GFP and growing exponentially were submitted to rapamycin treatment and inspected by fluorescence in live conditions following the addition of the drug (Fig. 6A). Drug treatment led to the rapid nucleolar enrichment of DIM2-GFP (Fig. 6A). RRP12-GFP was also rapidly concentrated within the nucleolus upon rapamycin treatment (data not shown). As described above, that both DIM2 and RRP12 concentrated within the nucleolus was confirmed on fixed cells by immunofluorescence with an anti-Nop1 antibody (Fig. 6B).

A direct demonstration that the TOR pathway is involved was obtained for DIM2 in cells that were either deleted for FPR1 (*fpr1::Δ*) or that expressed the semi-dominant *tor1-1* mutation (Fig. 6A). FPR1 encodes FKBP, a drug adaptor that presents rapamycin to the TORC1 complex, while the semi-dominant *tor1-1* allele carries a substitution that prevents the association of TORC1 with FKBP-rapamycin (for reviews, see Loewith and Hall 2004; Wullschleger et al. 2006). TOR kinases regulate cell growth temporally and spatially through their involvement in the TORC1 and TORC2 complexes, respectively; only TORC1 is sensitive to rapamycin and relevant to our analysis. Rapamycin treatment did not trigger the nucleolar localization of DIM2-GFP in *fpr1::Δ* or *tor1-1* cells, indicating that the TOR pathway is involved in this phenomenon.

Since the KH domain of DIM2 confers RNA binding capability, we were interested to test whether its absence would somehow affect the dynamic subcellular distribution of the protein. The KH domain is essential (Figs. 1, 2) and this possibility was thus tested in diploid yeast strains that expressed one allele of DIM2 either as a full-length GFP construct or a version shortened at position 203 (corresponding to the ΔC ter allele described above). The wild-type DIM2-GFP construct was concentrated in the nucleolus upon nutritional stress and was sensitive to rapamycin treatment (Fig. 6C), as discussed previously in haploid cells (Figs. 5, 6A). Deleting the KH domain of DIM2 significantly impaired its subcellular distribution: The truncated protein was nuclear enriched in exponentially growing cells, and neither nutritional stress nor rapamycin treatment led to any significant nucleolar enrichment (Fig. 6C).

The relocation to the nucleolus of DIM2 and RRP12 could be an indirect effect, merely reflecting an alteration in the steady-state level of the target protein. To exclude this possibility, the expression level of both GFP constructs was tested by Western blotting under growth conditions that triggered nucleolar entrapment (saturated cultures, rapamycin, and NaCl treatments, Supplemental Fig. S2). The steady-state levels of DIM2-GFP and RRP12-GFP were largely unaltered. The exception was the RRP12-GFP fusion in saturated cultures that could not be detected, owing to a severe transcriptional down-regulation (data not shown) and to its consistently increased sensitivity to degradation during the protein extraction procedure in these conditions.

DIM2 carries a putative NES sequence that is required for efficient pre-40S export

While mapping the KH-domain of DIM2, we noted that the protein carries a conserved stretch of leucine residues (positions 175–180) at its carboxyl-terminal end that scored positively as a putative NES signal when tested with a dedicated algorithm (Fig. 7A; la Cour et al. 2004). This prompted us to address the involvement of DIM2 in pre-40S export.

Following nucleolar cleavage at sites A_0–A_2, the 20S pre-rRNA is exported to the cytoplasm, where it is cleaved at site D to generate the 18S rRNA and the D-A_2 spacer byproduct (see Fig. 2B). In wild-type cells, the D-A_2 RNA is rapidly degraded by the 5′–3′ exoribonuclease XRN1 and is not normally detected (L. Wacheul and D.L.J. Lafontaine unpubl.). Thus, a probe specific to this RNA region can be used to study export of the small subunit.

To directly test the prediction that the putative NES sequence may function as a bona fide export motif, three mutations were generated that either deleted residues 175–180 (ΔNES) or substituted one or two conserved leucine residues for alanines (L177A and L177A L180A). As described above (Fig. 1), mutations in the putative NES

sequence were expressed from a low-copy plasmid as an amino-tagged ProtA fusion in *tet::dim2* cells. The presence of the ProtA epitope allowed us to establish that each construct was stably expressed (Fig. 7C; Supplemental Fig. S3B). Each mutation was tested for its effect on growth, pre-rRNA processing, and pre-40S export by transferring the cells in doxycycline-containing medium for 12 and 24 h (Fig. 7; Supplemental Fig. S3). Pre-40S export was analyzed by FISH with a Cy3-labeled probe specific to the 5′-end of ITS1 (Fig. 2B).

In an otherwise wild-type isogenic control strain, and in agreement with the subcellular distribution of pre-rRNA intermediates discussed above, the 5′-ITS1 FISH analysis revealed both a nuclear and a cytoplasmic signal (Fig. 7B,C). Depletion of endogenous DIM2 (Fig. 7C, EMPTY control construct) resulted in a severe depletion of the cytoplasmic signal (Fig. 7C, arrowhead) interpreted as inhibition in pre-40S export (Fig. 7B). At the intermediate depletion time point of 12 h, the nuclear detection showed
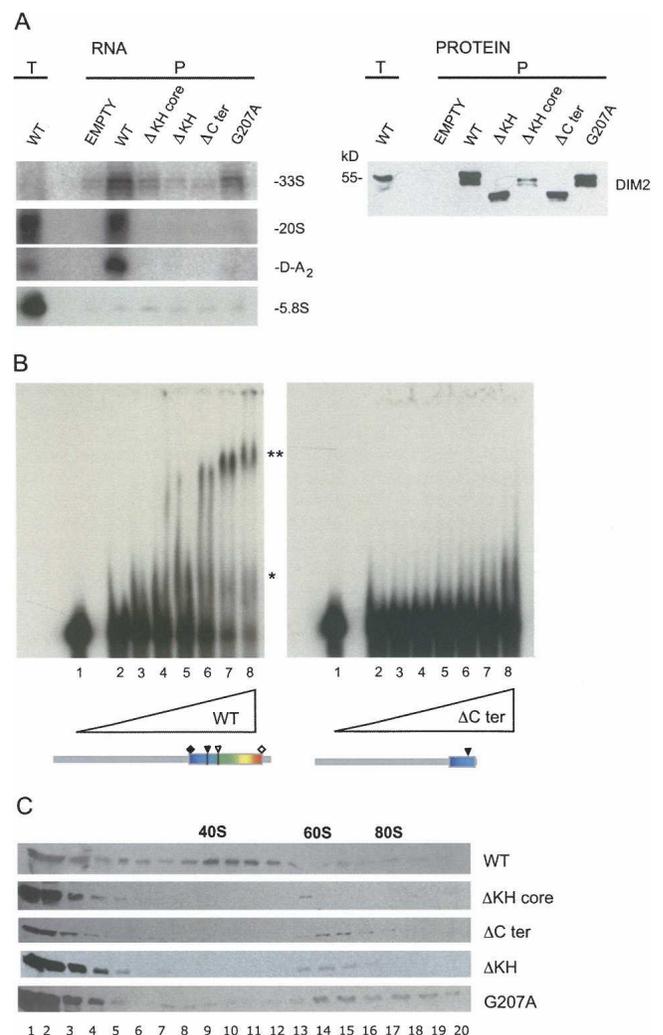

FIGURE 3. (Legend on next page)

a reduced nucleoplasmic signal resulting in an apparent nucleolar enrichment and a nucleoplasmic "trail" (Fig. 7B, closed arrowheads [see inset]). This indicates that DIM2 is required both for efficient pre-40S ribosome intranuclear transport and nucleocytoplasmic export. Expression of the ΔNES mutation also resulted in a severe pre-40S ribosome export defect (Fig. 7B); however, in this case the intranuclear distribution was not affected. The DIM2ΔNES mutation impacted growth and A_1–A_2 pre-rRNA processing in a fashion similar to that of DIM2 depletion (Supplemental Fig. S3). In contrast, substitution of one or two conserved leucines did not affect growth, pre-rRNA processing, or pre-40S export (Figs. 7B; Supplemental Fig. S3).

The ΔNES mutation was analyzed in closer details in a shorter depletion time course (Fig. 7C) to ask if export defects could be separated temporally from pre-rRNA processing inhibitions. Strikingly, transferring cells that expressed the DIM2ΔNES construct for periods as short as 1 h to doxycycline-containing medium was sufficient to detect a dramatic reduction in pre-40S export (Fig. 7C). At this time point, A_1–A_2 pre-rRNA processing was not detectably affected (Fig. 7C, right bottom panel, lane 2, no significant 22S accumulation). Depleting endogenous DIM2 for 1 h, corresponding to only approximately half a doubling time, did not significantly affect pre-40S export (Fig. 7C, EMPTY panels), A_1–A_2 pre-rRNA processing or growth (Fig. S3).

FIGURE 3. The KH domain of DIM2 binds the D-A_2 region of the pre-rRNA in vivo and in vitro. (*A*) Affinity purification analysis. Total extracts from yeast cells expressing the DIM2 constructs described in Figure 1 were subjected to affinity purification with IgG-coupled agarose beads. Copurifying RNAs were identified either by primer extension or Northern blotting (*left* panels). As a control, the presence of each bait protein in the pellet fractions was tested by Western blotting (*right* panel). (*Left* panels) RNA aliquots of the total (T) and pellet (P) fractions, loaded in a 1:10 ratio, were either processed by primer extension (33S detected with oligo a) or by Northern blots with separation in a 1.2% agarose/formaldehyde gel (20S) or in an 8% acrylamide/urea gel (D-A_2 and 5.8S). Gels were transferred to nylon membranes and hybridized in a Northern blot experiment. The 20S pre-rRNA and the D-A_2 spacer fragment were detected with probe b (Fig. 2B). As a control for specificity, a probe that selects the 5.8S rRNA (oligonucleotide d) that is not known to interact with DIM2 was used. (*Right* panel) Protein aliquots of the total (T) and pellet (P) fractions, loaded in a 1:10 ratio, were separated by SDS-PAGE and transferred for Western blotting with an antibody specific to the protein A moiety of the protein fusions. (*B*) Gel-shift assay. Increasing amounts (0–250 nM) of purified recombinant full-length GST-DIM2 and a version lacking the carboxyl-terminal KH domain were incubated with 10 fmol of gel-purified, radiolabeled, in vitro synthesized D-A_2 fragment and resolved on 5% acrylamide gels in nondenaturing conditions (see Materials and Methods). Shift (*) and supershift (**) are indicated. (*C*) Glycerol gradient analysis. Equivalent amounts of total extracts prepared from cells expressing the DIM2 constructs indicated were layered onto 10%–30% glycerol gradients and resolved by centrifugation. Twenty fractions were recovered, and total protein was extracted and analyzed by anti-ProtA Western blot.

DISCUSSION

The 40S ribosome synthesis factors DIM2 and RRP12 are nucleolar restricted under stressful growth conditions in a TOR-dependent fashion

Eukaryotic cell proliferation is controlled by specific growth factors and the availability of essential nutrients. In yeast, the stationary phase is a specialized nondividing state that cells enter when essential nutrients are missing (e.g., a suitable carbon source) (for reviews, see Werner-Washburne et al. 1996; Herman 2002). Entry into stationary phase is regulated by complex signal transduction pathways, including the evolutionarily conserved TOR cascade (for reviews, see Loewith and Hall 2004; Wullschleger et al. 2006). That the TOR pathway activates ribosome synthesis in yeast is evident from the observation that nutrient limitation, as well as addition of the immunosuppressive and antifungal drug rapamycin, a potent inhibitor of TOR, leads to the rapid extinction of the transcription of rRNA by Pol I, of ribosomal protein genes, and the Ribi Regulon (a set of coordinately expressed genes encoding ribosome synthesis factors) by Pol II and of 5S rRNA by Pol III (for review, see Powers et al. 2004). The involvement of the TOR cascade in this regulation involves alteration in the subcellular distribution of several transcription factors. TOR1 itself, which interacts with the 35S rDNA chromatin promoter and is critical for pre-rRNA synthesis, is dynamically distributed in the cytoplasm and the nucleus in yeast and is translocated to the cytoplasm in a nutrient-dependent and rapamycin-sensitive fashion (Li et al. 2006).

We have reported that the pre-40S ribosome synthesis factors DIM2 and RRP12 are specifically concentrated within the nucleolus under stressful growth conditions and that this localization requires the TOR pathway (Figs. 5, 6). Recently, Honma et al. (2006) reported the specific TOR-dependent nucleolar tethering of three large ribosome subunit synthesis factors, NOG1, NOP7, and RPL24, and suggested that TOR not only regulates ribosome synthesis at the level of production of its constituents but that it also regulates late steps of ribosome assembly. Our observations are fully compatible with this hypothesis and specifically address the 40S ribosome synthesis pathway. We do not believe that the relocation to the nucleolus of DIM2 and RRP12 merely reflects the drastic down-regulation of ribosome synthesis that occurs under nutrient starvation and various stressful growth conditions, because 10 other ribosome synthesis factors associated with closely related pre-40S particles were not affected in their subcellular distribution. Further, the steady-state levels of the DIM2 and RRP12 GFP constructs were tested under several conditions that stimulated nucleolar relocation and were found largely unaffected.
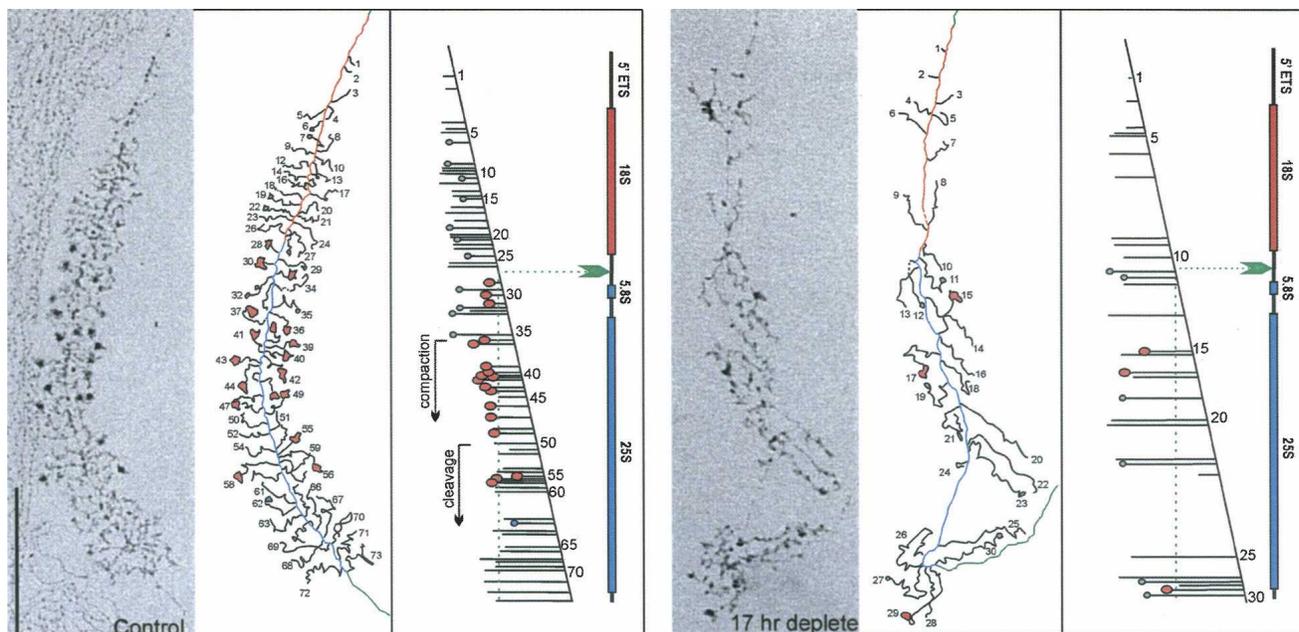
FIGURE 4. DIM2 is required for cotranscriptional ribosome assembly. Representative yeast rRNA genes are shown as visualized by chromatin spreading. *tet::dim2* cells were grown to mid-log phase in YPD (control) or YPD supplemented with doxycycline (17-h deplete) and spreads made according to Osheim et al. (2004). Interpretive tracing of the genes and transcript mapping are provided. DNA is color coded as follows: 5′ end to site A_2 in red, A_2 to 3′ end in blue, and the intergene spacer in green. Particles that appear on the transcripts are shown on the tracing as follows: gray particles correspond to the initial small 5′-terminal knobs, red to the mature SSU processomes, and blue to pre-large-subunit knobs that form at the 5′ end of cleaved transcripts. Scale bar is 0.5 μm.

DIM2 is required for efficient cotranscriptional ribosome assembly

We, and others, reported that DIM2 is required for early nucleolar pre-rRNA processing at sites A_1 and A_2 (Senapin et al. 2003; Vanrobays et al. 2004). Since ~50% of pre-rRNA molecules are cleaved cotranscriptionally within ITS1 (Osheim et al. 2004), we anticipated that these pre-rRNA processing inhibitions would severely affect cotranscriptional ribosome assembly kinetics. Indeed, chromatin spread inspection in cells depleted for DIM2 revealed a much reduced level of normal cotranscriptional cleavage, as well as an increase in aberrant cotranscriptional cleavage (Fig. 4). Further, failure to assemble DIM2 onto pre-ribosomes in a timely fashion led to significant decreases in deposition of 5′-ETS particles and in compaction and maturation of SSU processomes. The binding of DIM2 to the pre-rRNAs thus appears as a prerequisite step to downstream assembly reactions and is likely essential to generate a pre-rRNP whose conformation is compatible with pre-rRNA cleavage and pre-ribosome export.

The KH domain of DIM2 is required for RNA and pre-ribosome association

We have addressed the function in ribosome synthesis of the KH domain of DIM2 (Figs. 1, 2) and concluded that it confers RNA binding capability and that the protein binds the RNA directly at the D-A_2 spacer region of the pre-rRNAs. In the absence of a functional KH domain, DIM2 did not quantitatively interact with 90S pre-ribosomes and did not associate with the large nucleolar pre-rRNAs (Fig. 3). Interaction with pre-40S ribosomes and the cytoplasmic D-A_2 spacer fragment was also lost. Consistently, inactivation of the KH domain led to pre-rRNA processing inhibitions at cleavage sites A_1 and A_2, similar to those previously reported upon depletion of the protein (Vanrobays et al. 2004), and to alterations in the subcellular distribution of DIM2 (Fig. 6C). Interestingly, a single alanine substitution in the KH domain (G207A) was sufficient to inhibit cleavages at site A_1 and A_2 (accumulation of the 22S RNA) but with moderate effects on pre-ribosome association, the steady-state level of mature rRNA, and growth.

DIM2 is required for pre-40S ribosome export

Ribosome export operates through the recruitment to the ribosome synthesis pathway of general export factors by specific adaptors (see Introduction). For pre-60S ribosomes, the NES-containing NMD3 that associates with the exportin CRM1/XPO1 is one such adaptor (Ho et al. 2000; Gadal et al. 2001). For pre-40S, LTV1 has been proposed to act similarly (Seiser et al. 2006). However, LTV1 is not essential and can thus not account by itself for
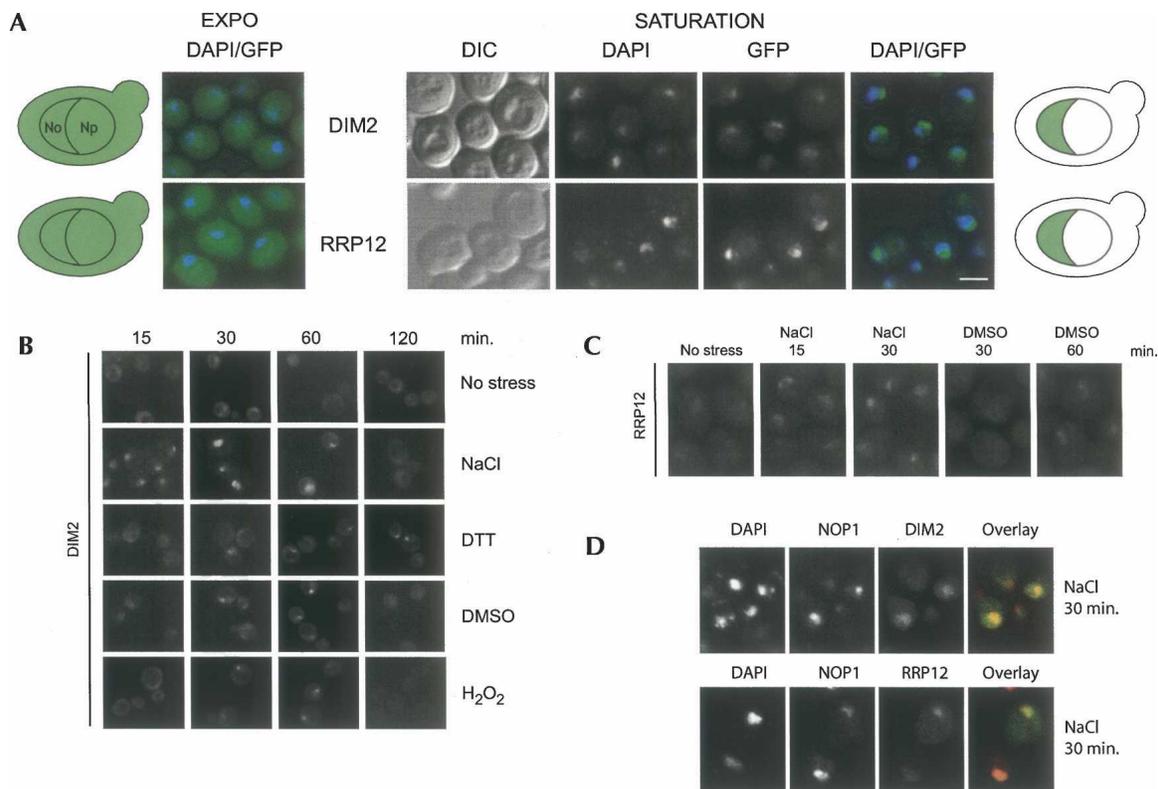
FIGURE 5. DIM2 and RRP12 are nucleolar-restricted upon nutritional, osmotic, and oxidative stress. (*A*) GFP fluorescence in fixed cells. Yeast cells expressing functional GFP constructs of DIM2 and RRP12 grown in complete glucose-based medium were observed by fluorescence in fast-growing conditions and in saturated cultures. Cells were collected at OD_{600} 0.3 (EXPO) and 2 d following the diauxic-shift (SATURATION). Both DIM2 and RRP12 showed a nucleolar staining facing the bulk DNA labeled with DAPI. As expected, mitochondrial DNA (cytoplasmic ring) was detected in cells from saturated cultures (best seen in the RRP12 panel). DIC, differential interference contrast; DAPI, DNA stain; GFP, green fluorescence. Summary cartoons to the *left* and *right*. No, nucleolus; Np, nucleoplasm. (*B,C*) GFP fluorescence in live cells. Hypertonic and oxidative stresses mimic the effect of nutrient deprivation on DIM2 and RRP12 nucleolar relocation. Fast-growing DIM2-GFP or RRP12-GFP cells were exposed to various stresses, including NaCl 0.5 M, DTT 2 mM, DMSO 10%, and H_2O_2 0.4 mM, and directly observed by GFP fluorescence at regular intervals. For each stress, a time course is illustrated. The crescent-shaped nucleolar labeling is easily scored. (*D*) Indirect immunofluorescence. Nucleolar sequestration was triggered by treating fast-growing yeast cells expressing DIM2-GFP or RRP12-GFP with NaCl for 30 min. Spheroplasts were decorated with an anti-Nop1 antibody and counterstained with DAPI.

all pre-40S export. The presence of a putative NES sequence at the carboxyl-terminal end of DIM2 suggested that it may specifically contribute to this process. Depletion of DIM2 indeed strongly affected pre-40S ribosome export (Fig. 7). DIM2 depletion also affected the intranuclear distribution of pre-40S ribosomes. Single and double substitution of conserved amino acid residues within the putative NES, however, did not affect pre-40S export while obliteration of the NES sequence inhibited export but also impaired pre-rRNA processing. In the case of NMD3, mutating individual or multiple leucine residues in the NES was also generally well tolerated (Hedges et al. 2006).

In conclusion, failure to assemble DIM2 onto nascent ribosomal transcripts leads to pre-rRNA processing inhibitions and cotranscriptional ribosome assembly defects that inhibit pre-ribosome nucleolar release and nucleocytoplasmic translocation through the NPC. We would also like to suggest that, in addition to its function in ribosome assembly, DIM2 plays a more direct role in ribosome

export since the expression of a construct that precisely lacks the NES motif severely impacted pre-40S ribosome export under conditions where no pre-rRNA processing defects could be scored (early depletion). The intranuclear distribution of pre-40S ribosomes was also not perturbed in the ΔNES mutant. These observations clearly do not formally demonstrate that the putative NES is an active motif but do indicate that the DIM2ΔNES construct exerts a dominant negative effect on pre-40S export. Particularly relevant to a possible more direct involvement of DIM2 in pre-40S export is its reported interaction with the FG-repeats nucleoporin NUP116 (Rout et al. 2000), which localizes on both sides of the NPC and interacts with the mRNA and pre-60S ribosome export factor MEX67 (Strawn et al. 2001; Yao et al. 2007, 2008).

The HEAT-repeats/Armadillo RRP12 protein that, with DIM2 and other 40S ribosome synthesis factors, defines a structural and functional "neighborhood" within pre-40S ribosomes, is required for export of both ribosomal
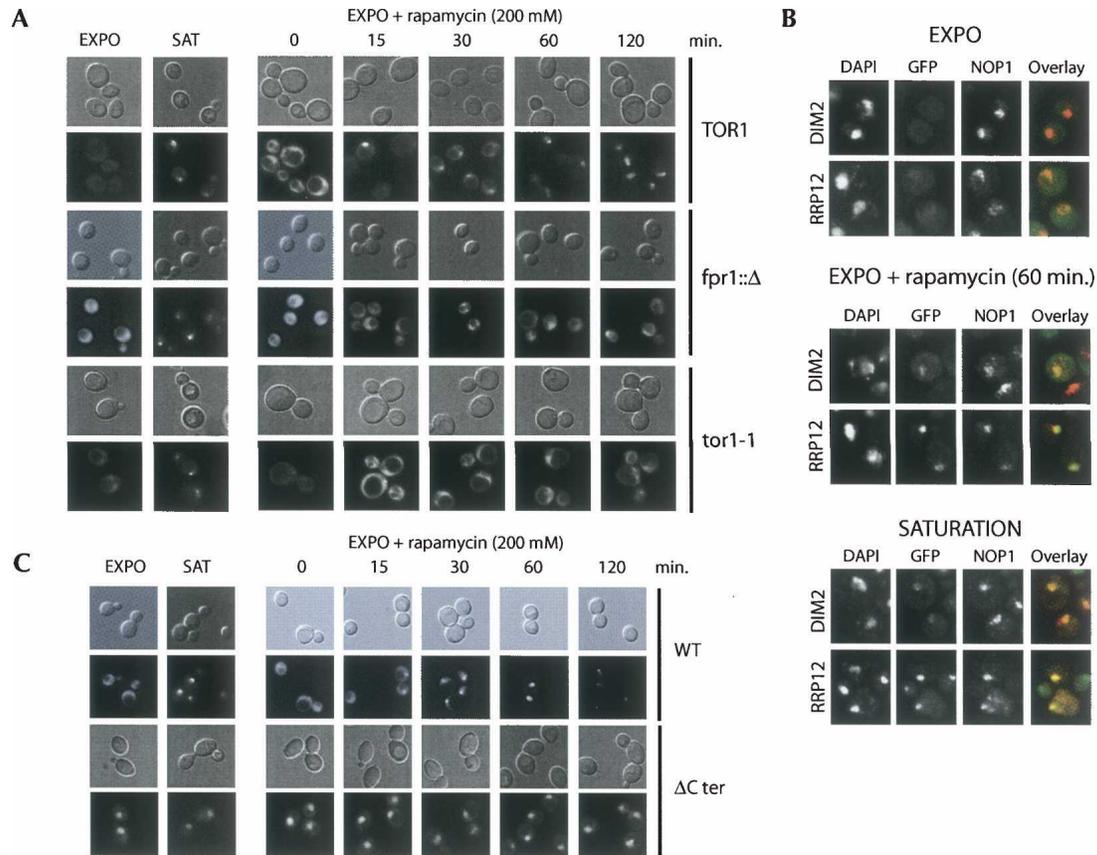
FIGURE 6. The nucleolar entrapment of DIM2 and RRP12 is under TOR control. (*A*) GFP fluorescence in live cells. DIM2-GFP cells expressing either a wild-type (TOR1) or a semi-dominant (*tor1-1*) allele of TOR1 or carrying a deletion in FPR1 (*fpr1::Δ*) were cultured to mid log-phase (OD$_{600}$ ~0.3), exposed to 200 mM rapamycin for up to 2 h and directly observed by GFP fluorescence at the time points indicated (*right* panels). Both *fpr1::Δ* and *tor1-1* cells were resistant to rapamycin in a drop plate assay (data not shown). As a control, all strains were grown to saturation (2 d post-diauxic shift) in the absence of rapamycin treatment (*left* panels). The crescent-shaped staining indicative of nucleolar localization was easily scored. EXPO, fast growing yeast cells; SAT, saturated cultures. For the time points for each condition, the *upper* photos are differential interference contrast and the *lower* photos are fluorescence micrographs. (*B*) Indirect immunofluorescence. DIM2-GFP and RRP12-GFP cells were either grown exponentially (OD$_{600}$ ~0.3), grown exponentially and exposed to rapamycin treatment for 60 min, or grown to saturation. They were then processed in an immunofluorescence experiment with an antibody specific to the fibrillarin (mA66 against yeast Nop1, see Materials and Methods), which was decorated in red. (*C*) GFP fluorescence in live cells. In the absence of a functional KH domain the subcellular distribution and trafficking of DIM2-GFP is affected. Diploid cells expressing either a full-length carboxyl GFP version of DIM2 (WT) or a version carrying a truncation of the KH domain (ΔC ter) were cultured in complete medium and imaged by fluorescence in fast-growing yeast cells (OD$_{600}$ ~0.3, EXPO) and in saturated cultures (2 d post-diauxic shift, SAT) (*left* panels). In parallel, exponentially growing cells were exposed to a final concentration of 200 mM rapamycin for the time points indicated (*right* panels).

subunits and also interacts with NUP116 (Oeffinger et al. 2004). We found it quite striking that the two proteins identified here as nucleolar restricted under suboptimal growth conditions are required for pre-ribosome export. The involvement of TOR in this nucleolar tethering further suggests that ribosome export is a step in the ribosome assembly pathway that likely evolved a regulatory target for this signaling cascade.

MATERIALS AND METHODS

Yeast media

Yeast cells were grown according to standard procedures in YPD (2% peptone, 1% yeast extract, 2% glucose) and glucose-based (2%) selective synthetic media. For stress induction, rapamycin was used at a final concentration of 200 nM, NaCl at 0.5 M, DTT at 2 mM, DMSO at 10%, and H$_2$O$_2$ at 0.4 mM. For DIM2 depletion, doxycycline was added at a final concentration of 10 μg/mL.

Yeast strains

Yeast strains are summarized in Supplemental Table 2.

Plasmids

Plasmids are listed in Supplemental Table 1. A DNA fragment encoding DIM2 was generated by PCR using oligos 5′-YOR145C and 3′-YOR145C and cloned as Bam HI/Nde I in plasmid pProtA generating plasmid pProtA-DIM2 (pDL0399). KH and NES mutations were generated by a two-step PCR
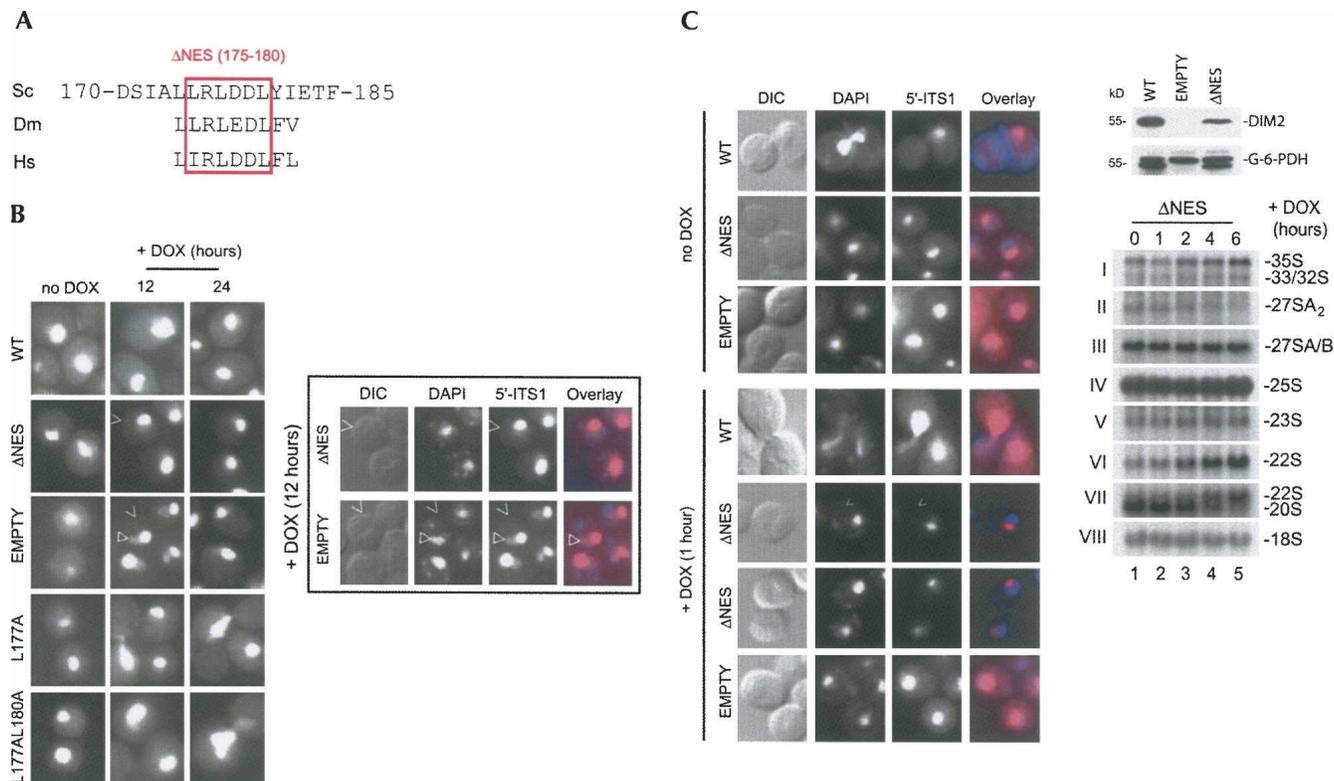
FIGURE 7. DIM2 contains a putative NES sequence and is required for pre-40S ribosome export. (*A*) DIM2 carries an evolutionarily conserved putative leucine-rich NES. Sc, *Saccharomyces cerevisiae*; Dm, *Drosophila melanogaster*; Hs, *Homo sapiens*. (*B*) Pre-40S ribosomes visualization by FISH in mutants in the putative NES. Depletion of endogenous DIM2 was achieved by transferring *tet::dim2* cells transformed with a wild-type full-length construct (WT), an empty control plasmid, or constructs expressing either a precise deletion of the putative NES (ΔNES) or versions with alanine substitutions in conserved residues (L177A and L177AL180A) in doxycycline-containing medium for 12 and 24 h. All panels shown were hybridized with a Cy3-labeled 5′-ITS1 probe (oligo LD597). Arrowheads point to the cytoplasm; closed arrowhead points to nucleoplasm. (*Inset*) The 12 h depletion time point is shown with differential interference contrast (DIC), DNA stain (DAPI), and overlay. (*C*) Detailed functional characterization of the ΔNES mutation. The expression of a DIM2 construct that precisely lacks the six amino acid residues that encompass the putative NES was sufficient to severely inhibit pre-40S export in conditions that did not significantly affect pre-rRNA processing. (*Left* panels) Pre-rRNAs were visualized as in panel *B*. Depletion of endogenous DIM2 was achieved for 1 h. Arrowhead points to the cytoplasm. (*Right top* panels) The ΔNES construct is stably expressed. Equivalent amount of total protein extracted in the absence of doxycycline-induced depletion was loaded in each lane and tested by anti-ProtA Western blot analysis. As a loading control, the membrane was probed with an antibody specific to G-6-PDH. (*Right bottom* panels) Depleting endogenous DIM2 for 1 h did not result in any significant pre-rRNA processing inhibitions at sites A_1–A_2. Pre-rRNA processing analysis was conducted as described in Figure 2.

strategy (see Supplemental Table 4 for oligonucleotide sequences), introduced in pDL0399, sequenced to the nucleotide, and transformed in *tet::dim2* cells (YDL801). pVL21 (pGST-DIM2) and pVL25 (pGST-DIM2ΔC ter) were cloned as EcoRI/XmaI fragments from pProtA-DIM2 (pDL0399) and pProtA-DIM2ΔC (pDL0401), respectively, in plasmid pGEX5-1 (GE Healthcare).

Western blot analysis

Total protein extracts were separated by SDS-PAGE and transferred to hybond-C membranes (GE Healthcare). ProtA- and TAP-tagged proteins were detected with the peroxidase-antiperoxidase soluble complex (PAP; Sigma P2026) used at 1:1000 for an hour at room temperature. GFP detection was with a specific anti-GFP mouse antibody (GFP-20; Sigma G6539) followed by a goat anti-mouse-HRP (Santa Cruz; SC2005), both used at 1:1000 at room temperature for 1 h. As loading controls, membranes were probed with anti-glucose-6-phosphate dehydro-

genase raised in rabbit (G-6-PDH; Sigma; A9521) used at 1:2500 for 2 h followed by incubation at 1:1000 for 1 h at room temperature with a anti rabbit IgG-HRP raised in donkey (Santa Cruz; SC2313).

Glycerol gradients

Total protein extracts and sedimentation profiles on 10%–30% glycerol gradients were prepared as described previously (Vanrobays et al. 2004).

Affinity purification

Affinity purification on IgG-coated agarose beads (Sigma A2909) was as described previously (Vanrobays et al. 2004).

Northern blot analysis and primer extension

Total RNA was extracted according to a standard phenol/chloroform procedure (Lafontaine et al. 1995) and either separated on

1.2% agarose/formaldehyde or 8% acrylamide gels. Oligonucleotides used in the Northern blot hybridizations and primer extension analysis are described in Supplemental Table 3.

Protein expression and purification

Glutathione S-transferase (GST) DIM2 constructs were purified from *Escherichia coli* BL21 cells carrying pVL21 (pT7-GST-DIM2) or pVL25 (pT7-GST-DIM2ΔCter). Protein expression was induced with 1 mM isopropyl-β-D-thiogalactopyranoside (IPTG) for 4 h at 37°C and purified by affinity chromatography using glutathione agarose beads according to the manufacturer's instructions (Sigma).

Gel-shift assays

A DNA fragment encoding the D-A$_2$ region of the rDNA was generated by PCR with oligonucleotides LD465 and LD466 and plasmid HW10 (Henry et al. 1994). Oligo LD465 contains a minimal T7 promoter sequence allowing in vitro RNA synthesis. The radiolabeled RNA transcript was gel purified on acrylamide gels, resuspended in 30 mM Tris-HCl (pH 7.4), 150 mM KCl, 2 mM MgCl$_2$ buffer, heat denatured at 70°C for 10 min, followed by slow cooling to room temperature. Ten femtomoles of RNA substrate were incubated with increasing amounts of purified protein (ranging from 5 to 500 nM), in 30 mM Tris-HCl (pH 7.4), 150 mM KCl, 2 mM MgCl$_2$, 0.1% Triton X-100, 1 mM DTT, 20% glycerol, 0.2% BSA, incubated for 12 min at room temperature, and resolved in 8% TBE 0.5×/glycerol 5% polyacrylamide.

Fluorescence data

Fluorescence data were generated on a Zeiss Axio Imager Z1 equipped with a 100× objective (N.A. of 1.46) and standard filter sets. Images were captured with a Zeiss HRm CCD camera and the native Axiovision 4.5 software, transferred to Photoshop CS3 and Illustrator CS3 (Adobe). Unless otherwise stated, cells were washed once for 5 min in PBS 1×/formaldehyde 3.7% and three times in PBS 1× successively. Mounting media with DAPI (Vectashield) and poly-lysine Teflon-coated slides were used. Standard immunofluorescence (Pringle et al. 1991) was used for the detection of the prototypic nucleolar protein NOP1. Cells were spheroplasted and incubated successively for 2 h at room temperature with a mouse monoclonal anti-NOP1 antibody at 1:500 (mA66, a gift from J. Aris, University of Florida) and a goat anti-mouse IgG coupled to Alexa594 at 1:1000 (Molecular Probes, A-11005).

FISH analysis

FISH analysis was performed according to the Singer Lab protocol (http://singerlab.aecom.yu.edu/). Cy3-labeled 5′-ITS1 probe was oligonucleotide LD597 (see Supplemental Table 3).

Chromatin spreads

Chromatin spreads were performed according to Osheim et al. (2004).

Bioinformatics

Bioinformatics: DIM2 (also known as RRP20 and PNO1) is YOR145C. The putative DIM2 NES was identified at http://

www.cbs.dtu.dk/services/NetNES. Multiple alignments were performed with Multalin at http://bioinfo.genopole-toulouse.prd.fr/multalin/multalin.html. Folding prediction of the KH domain was realized at http://www.predictprotein.org/ and http://swissmodel.expasy.org/ based on the 1.5Å crystal structure of an Archaeal homolog found in *Aeropyrum pernix*. The prediction was visualized using a Pdb viewer.

SUPPLEMENTAL DATA

Supplemental material can be found at http://www.rnajournal.org.

ACKNOWLEDGMENTS

REFERENCES

Bradatsch, B., Katahira, J., Kowalinski, E., Bange, G., Yao, W., Sekimoto, T., Baumgartel, V., Boese, G., Bassler, J., Wild, K., et al. 2007. Arx1 functions as an unorthodox nuclear export receptor for the 60S preribosomal subunit. *Mol. Cell* **27:** 767–779.

Fatica, A. and Tollervey, D. 2002. Making ribosomes. *Curr. Opin. Cell Biol.* **14:** 313–318.

Fromont-Racine, M., Senger, B., Saveanu, C., and Fasiolo, F. 2003. Ribosome assembly in eukaryotes. *Gene* **313:** 17–42.

Gadal, O., Strauss, D., Kessl, J., Trumpower, B., Tollervey, D., and Hurt, E. 2001. Nuclear export of 60s ribosomal subunits depends on Xpo1p and requires a nuclear export sequence-containing factor, Nmd3p, that associates with the large subunit protein Rpl10p. *Mol. Cell. Biol.* **21:** 3405–3415.

Garcia-Mena, J., Das, A., Sanchez-Trujillo, A., Portier, C., and Montanez, C. 1999. A novel mutation in the KH domain of polynucleotide phosphorylase affects autoregulation and mRNA decay in *Escherichia coli*. *Mol. Microbiol.* **33:** 235–248.

Grishin, N.V. 2001. KH domain: One motif, two folds. *Nucleic Acids Res.* **29:** 638–643.

Hedges, J., Chen, Y.I., West, M., Bussiere, C., and Johnson, A.W. 2006. Mapping the functional domains of yeast NMD3, the nuclear export adapter for the 60 S ribosomal subunit. *J. Biol. Chem.* **281:** 36579–36587.

Henras, A.K., Soudet, J., Gerus, M., Lebaron, S., Caizergues-Ferrer, M., Mougin, A., and Henry, Y. 2008. The post-transcriptional steps of eukaryotic ribosome biogenesis. *Cell Mol. Life Sci.* doi: 10.1007/s00018-008-8027-0.

Henry, Y., Wood, H., Morrissey, J.P., Petfalski, E., Kearsey, S., and Tollervey, D. 1994. The 5′ end of yeast 5.8S rRNA is generated by exonucleases from an upstream cleavage site. *EMBO J.* **13:** 2452–2463.

Herman, P.K. 2002. Stationary phase in yeast. *Curr. Opin. Microbiol.* **5:** 602–607.

Ho, J.H., Kallstrom, G., and Johnson, A.W. 2000. Nmd3p is a Crm1p-dependent adapter protein for nuclear export of the large ribosomal subunit. *J. Cell Biol.* **151:** 1057–1066.

Honma, Y., Kitamura, A., Shioda, R., Maruyama, H., Ozaki, K., Oda, Y., Mini, T., Jeno, P., Maki, Y., Yonezawa, K., et al. 2006. TOR regulates late steps of ribosome maturation in the nucleoplasm via Nog1 in response to nutrients. *EMBO J.* **25:** 3832–3842.

Hung, N.J., Lo, K.Y., Patel, S.S., Helmke, K., and Johnson, A.W. 2008. Arx1 is a nuclear export receptor for the 60S ribosomal subunit in yeast. *Mol. Biol. Cell* **19:** 735–744.

Jia, M.Z., Ohtsuka, J., Lee, W.C., Nagata, K., and Tanokura, M. 2007. Crystal structure of Dim2p: A preribosomal RNA processing factor, from *Pyrococcus horikoshii* at 2.30 Å. *Proteins* **69:** 428–432.

Jones, A.R. and Schedl, T. 1995. Mutations in gld-1, a female germ cell-specific tumor suppressor gene in *Caenorhabditis elegans*, affect a conserved domain also found in Src-associated protein Sam68. *Genes & Dev.* **9:** 1491–1504.

Jorgensen, P., Tyers, M., and Warner, J.R. 2004. Forging the factory: Ribosome synthesis and growth control in budding yeast. In *Cell growth: Control of cell size* (eds. M.N. Hall et al.), pp. 329–370. Cold Spring Harbor Laboratory Press, Cold Spring Harbor, NY.

Kufel, J., Allmang, C., Petfalski, E., Beggs, J., and Tollervey, D. 2003. Lsm Proteins are required for normal processing and stability of ribosomal RNAs. *J. Biol. Chem.* **278:** 2147–2156.

la Cour, T., Kiemer, L., Molgaard, A., Gupta, R., Skriver, K., and Brunak, S. 2004. Analysis and prediction of leucine-rich nuclear export signals. *Protein Eng. Des. Sel.* **17:** 527–536.

Lafontaine, D.L.J. 2004. Eukaryotic ribosome synthesis. In *Protein synthesis and ribosome structure* (ed. K. Nierhaus), pp. 107–143. Wiley-InterScience, New York.

Lafontaine, D., Vandenhaute, J., and Tollervey, D. 1995. The 18S rRNA dimethylase Dim1p is required for pre-ribosomal RNA processing in yeast. *Genes & Dev.* **9:** 2470–2481.

Lebreton, A., Saveanu, C., Decourty, L., Rain, J.C., Jacquier, A., and Fromont-Racine, M. 2006. A functional network involved in the recycling of nucleocytoplasmic pre-60S factors. *J. Cell Biol.* **173:** 349–360.

Lewis, H.A., Musunuru, K., Jensen, K.B., Edo, C., Chen, H., Darnell, R.B., and Burley, S.K. 2000. Sequence-specific RNA binding by a Nova KH domain: Implications for paraneoplastic disease and the fragile X syndrome. *Cell* **100:** 323–332.

Li, H., Tsang, C.K., Watkins, M., Bertram, P.G., and Zheng, X.F. 2006. Nutrient regulates Tor1 nuclear localization and association with rDNA promoter. *Nature* **442:** 1058–1061.

Loewith, R. and Hall, M.N. 2004. TOR signaling in yeast: Temporal and spatial control of cell growth. In *Cell growth: Control of cell size* (eds. M.N. Hall et al.), pp. 139–165. Cold Spring Harbor Laboratory Press, Cold Spring Harbor, NY.

Oeffinger, M., Dlakic, M., and Tollervey, D. 2004. A pre-ribosome-associated HEAT-repeat protein is required for export of both ribosomal subunits. *Genes & Dev.* **18:** 196–209.

Osheim, Y.N., French, S.L., Keck, K.M., Champion, E.A., Spasov, K., Dragon, F., Baserga, S.J., and Beyer, A.L. 2004. Pre-18S ribosomal RNA is structurally compacted into the SSU processome prior to being cleaved from nascent transcripts in *Saccharomyces cerevisiae*. *Mol. Cell* **16:** 943–954.

Powers, T., Dilova, I., Chen, C.Y., and Wedaman, K. 2004. Yeast TOR signaling: A mechanism for metabolic regulation. *Curr. Top. Microbiol. Immunol.* **279:** 39–51.

Pringle, J.R., Adams, A.E., Drubin, D.G., and Haarer, B.K. 1991. Immunofluorescence methods for yeast. *Methods Enzymol.* **194:** 565–602.

Rout, M.P., Aitchison, J.D., Suprapto, A., Hjertaas, K., Zhao, Y., and Chait, B.T. 2000. The yeast nuclear pore complex: Composition, architecture, and transport mechanism. *J. Cell Biol.* **148:** 635–651.

Seiser, R.M., Sundberg, A.E., Wollam, B.J., Zobel-Thropp, P., Baldwin, K., Spector, M.D., and Lycan, D.E. 2006. Ltv1 is required for efficient nuclear export of the ribosomal small subunit in *Saccharomyces cerevisiae*. *Genetics* **174:** 679–691.

Senapin, S., Clark-Walker, G.D., Chen, X.J., Seraphin, B., and Daugeron, M.C. 2003. RRP20, a component of the 90S preribosome, is required for pre-18S rRNA processing in *Saccharomyces cerevisiae*. *Nucleic Acids Res.* **31:** 2524–2533.

Stevens, A., Hsu, C.L., Isham, K.R., and Larimer, F.W. 1991. Fragments of the internal transcribed spacer 1 of pre-rRNA accumulate in *Saccharomyces cerevisiae* lacking 5′–3′ exoribonuclease 1. *J. Bacteriol.* **173:** 7024–7028.

Strawn, L.A., Shen, T., and Wente, S.R. 2001. The GLFG regions of Nup116p and Nup100p serve as binding sites for both Kap95p and Mex67p at the nuclear pore complex. *J. Biol. Chem.* **276:** 6445–6452.

Tschochner, H. and Hurt, E. 2003. Pre-ribosomes on the road from the nucleolus to the cytoplasm. *Trends Cell Biol.* **13:** 255–263.

Vanrobays, E., Gélugne, J.-P., Caizergues-Ferrer, M., and Lafontaine, D.L.J. 2004. Dim2p, a KH-domain protein required for small ribosomal subunit synthesis. *RNA* **10:** 645–656.

Weis, K. 2007. The nuclear pore complex: Oily spaghetti or gummy bear? *Cell* **130:** 405–407.

Werner-Washburne, M., Braun, E.L., Crawford, M.E., and Peck, V.M. 1996. Stationary phase in *Saccharomyces cerevisiae*. *Mol. Microbiol.* **19:** 1159–1166.

Wullschleger, S., Loewith, R., and Hall, M.N. 2006. TOR signaling in growth and metabolism. *Cell* **124:** 471–484.

Yao, W., Roser, D., Kohler, A., Bradatsch, B., Bassler, J., and Hurt, E. 2007. Nuclear export of ribosomal 60S subunits by the general mRNA export receptor Mex67-Mtr2. *Mol. Cell* **26:** 51–62.

Yao, W., Lutzmann, M., and Hurt, E. 2008. A versatile interaction platform on the Mex67-Mtr2 receptor creates an overlap between mRNA and ribosome export. *EMBO J.* **27:** 6–16.

Zemp, I. and Kutay, U. 2007. Nuclear export and cytoplasmic maturation of ribosomal subunits. *FEBS Lett.* **581:** 2783–2793.

Zhou, Y., Mah, T.F., Greenblatt, J., and Friedman, D.I. 2002. Evidence that the KH RNA-binding domains influence the action of the *E. coli* NusA protein. *J. Mol. Biol.* **318:** 1175–1188.